Title

Using Free-Breathing MRI to Quantify Pancreatic Fat and Investigate Spatial Heterogeneity in Children

Journal

Journal of Magnetic Resonance Imaging, 57(2)

ISSN

1053-1807

Authors

Story, Jacob D
Ghahremani, Shahnaz
Kafali, Sevgi Gokce
et al.

Publication Date

2023-02-01

DOI

10.1002/jmri.28337

Peer reviewed

HHS Public Access

Author manuscript

J Magn Reson Imaging. Author manuscript; available in PMC 2024 February 01.

Published in final edited form as:

J Magn Reson Imaging. 2023 February ; 57(2): 508–518. doi:10.1002/jmri.28337.

Using Free-Breathing MRI to Quantify Pancreatic Fat and Investigate Spatial Heterogeneity in Children

Jacob D. Story, BS[1], **Shahnaz Ghahremani, MD**[2], **Sevgi Gokce Kafali, MS**[2,3], **Shu-Fu Shih, MS**[2,3], **Kelsey J. Kuwahara, BS**[1], **Kara L. Calkins, MD**[4], **Holden H. Wu, PhD**[2,3,*]

[1]David Geffen School of Medicine, University of California Los Angeles, Los Angeles, CA, United States.

[2]Department of Radiological Sciences, David Geffen School of Medicine, University of California Los Angeles, Los Angeles, CA, United States.

[3]Department of Bioengineering, University of California Los Angeles, Los Angeles, CA, United States.

[4]Department of Pediatrics, Division of Neonatology and Developmental Biology, and the UCLA Children's Discovery and Innovation Institute, University of California Los Angeles, Los Angeles, CA, United States.

Abstract

Background: MRI acquisition for pediatric pancreatic fat quantification is limited by breath-holds (BH). Full segmentation (FS) or small region of interest (ROI) analysis methods may not account for pancreatic fat spatial heterogeneity, which may limit accuracy.

Purpose: To improve MRI acquisition and analysis for quantifying pancreatic proton-density fat fraction (pPDFF) in children by investigating free-breathing (FB)-MRI, characterizing pPDFF spatial heterogeneity, and relating pPDFF to clinical markers.

Study Type: Prospective.

Population: 34 children, including healthy (N=16, 8 female) and overweight (N=18, 5 female) subjects.

Field Strength and Sequences: 3T; multi-echo gradient-echo 3D stack-of-stars FB-MRI, multi-echo gradient-echo 3D Cartesian BH-MRI.

Assessment: A radiologist measured FS-based and ROI-based pPDFF on FB-MRI and BH-MRI PDFF maps, with anatomical images as references. Regional pPDFF in the pancreatic head, body, and tail were measured on FB-MRI. FS-pPDFF, ROI-pPDFF, and regional pPDFF were compared, and related to clinical markers, including hemoglobin A1c.

Statistical Tests: T-test, Bland-Altman analysis, Lin's concordance correlation coefficient (CCC), one-way analysis of variance, and Spearman's rank correlation coefficient were used. $P<0.05$ was considered significant.

*Correspondence to: Holden H. Wu, Ph.D., Department of Radiological Sciences, 300 UCLA Medical Plaza, Suite B119, Los Angeles, CA 90095, HoldenWu@mednet.ucla.edu.

Results: FS-pPDFF and ROI-pPDFF from FB-MRI and BH-MRI had mean difference = 0.4%; CCC was 0.95 for FS-pPDFF and 0.62 for ROI-pPDFF. FS-pPDFF was higher than ROI-pPDFF (10.4±6.4% vs. 4.2±2.8%). Tail-pPDFF (11.6±8.1%) was higher than body-pPDFF (8.9±6.3%) and head-pPDFF (8.7±5.2%). Head-pPDFF and body-pPDFF positively correlated with hemoglobin A1c.

Data Conclusion: FB-MRI pPDFF is comparable to BH-MRI. Spatial heterogeneity affects pPDFF quantification. Regional measurements of pPDFF in the head and body were correlated with hemoglobin A1c, a marker of insulin sensitivity.

INTRODUCTION

Pediatric obesity and diabetes mellitus are global health problems.[1] Pancreatic fat is a biomarker for identifying and understanding metabolic dysfunction in children.[2–7] While multiple methods for pancreatic fat quantification have been utilized, MRI is considered the reference standard as it has high inter-reader agreement and better visualization of deep organs compared to ultrasound.[8] Furthermore, MRI avoids ionizing radiation associated with X-ray computed tomography (CT).[8]

Proton-density fat fraction (PDFF) is an MRI parameter that has previously been validated for hepatic fat quantification and has more recently been applied to the pancreas.[9 10] However, using MRI to measure pancreatic fat in children is challenging because of image acquisition and analysis issues. Conventional breath-holding (BH) Cartesian MRI of the abdomen is limited by the scan duration for which subjects can hold their breath (typically 20 seconds or less), which can lead to decreased resolution or spatial coverage. Moreover, involuntary respiratory motion frequently impacts MR images in children and leads to image artifacts and spatial misregistration, degrading image quality and quantification accuracy.[11, 12]

Recently developed free-breathing (FB) 3D radial stack-of-stars abdominal MRI methods remove the need for BH and allow for increased spatial coverage and improved robustness to motion artifacts.[13, 14] In children, image quality of FB-MRI has been shown to be equivalent or superior to image quality of BH-MRI for assessing liver fat content.[15, 16] A different FB-MRI method (eXtra-Dimensional Golden-angle RAdial Sparse Parallel [XD-GRASP]) has also been shown to produce higher quality T_1-weighted pancreatic images than BH-MRI in adults, but it was not investigated for multi-echo MRI and fat quantification.[17] FB-MRI has yet to be applied to pancreatic fat quantification in the pediatric population.

Numerous image analysis methods have been used to estimate pancreatic PDFF (pPDFF) from MRI.[3–4, 7, 10, 18–22] A commonly used method involves placing several small oval regions of interest (ROIs) on the pancreas. Typically, this involves placing 1-cm^2 ROIs in the pancreatic head, body, and tail for a total of 3 ROIs, but the size, location, and quantity of ROIs varies in different studies.[3–4,7,18–22] Kato *et al.* suggested that numerous small ROIs poorly estimated pPDFF in adults due to sampling bias.[10] This is in contrast to the full segmentation (FS) method that contours the entire pancreas in all slices where the pancreas is visible.[10] Some data indicate that FS pPDFF measurement has higher inter- and intra-reader agreement compared to small ROI methods because the entire organ is

included.[10] However, contouring the entire pancreas may be a more time-consuming process than placing 3 small ROIs. Furthermore, due to the complex anatomy of the pancreas, even experienced radiologists may struggle with identifying the borders of the pancreas at all axial levels, and variations in what tissue is included may reduce reliability. For example, the long and narrow shape of the pancreas makes it susceptible to signal contamination from surrounding visceral fat due to respiratory motion in traditional BH-MRI.[23] A retrospective analysis involving FS contours in pediatric BH-MRI revealed significant intra-reader variation.[24]

While pancreatic steatosis is frequently implicated in the pathogenesis of diabetes and obesity, the literature is contradictory. Some studies have associated pPDFF with body mass index (BMI) and body weight, but other studies have failed to replicate these results.[3–7, 10] The relationship between pPDFF and beta-cell function, fasting insulin levels, and diabetes status is also unclear.[2–7, 9] These discrepancies may be because of the various pitfalls associated with the image analysis method used to measure pPDFF. An investigation that separately analyzed pPDFF of the pancreatic head versus the body/tail found that low-density lipoprotein (LDL) only correlated with pPDFF of the head, but not with pPDFF of the entire pancreas or of the body and tail.[10] The FS method measures pPDFF as an average over the entire organ. Thus, local variations between anatomic regions may be given more or less weight depending on their relative volumes. In contrast, small ROI methods typically sample from several regions (e.g., head, body, tail) with equal weighting despite their unequal overall volumes. Therefore, the method employed to measure pancreatic steatosis may influence the study's results. Determining the advantages of one method over another or investigating how a specific method could better address this limitation requires a more thorough knowledge of how fat is spatially distributed throughout the pancreas.

The aims of this study were to improve the acquisition and analysis of MRI for quantifying pPDFF in children by investigating FB-MRI in comparison to BH-MRI, characterizing spatial variations of pPDFF between anatomic regions in the pancreas using FB-MRI, and correlating pPDFF to anthropometric measurements and laboratory markers of metabolic dysfunction.

MATERIALS AND METHODS

Study Population

In this Health Insurance Portability and Accountability Act (HIPAA)-compliant and Institutional Review Board-approved prospective cohort study, healthy and overweight children between 6–17 years old were recruited. Parental permission was obtained and, when applicable, minor assent was also obtained. The overweight cohort included children with a BMI of ≥85th percentile.[25] All children in the overweight cohort also had suspected or diagnosed non-alcoholic fatty liver disease (NAFLD). Prediabetes or diabetes mellitus type 2 (DM2) status were also recorded. Prediabetes was defined as hemoglobin A1c of 5.7–6.4% and DM2 was defined as hemoglobin A1c ≥6.5%.[26] The healthy control cohort included children with a BMI <85th percentile. Exclusion criteria for both cohorts included congenital liver malformations, liver infections, pregnancy, inborn errors of metabolism, or MRI contraindications such as metallic objects in the body or

claustrophobia. Anthropometric measurements were performed at the research visit. Clinical data were collected through chart review. A research electronic data capture (REDCap) database was used for data management.[27]

Abdominal MRI

All subjects underwent a research exam with conventional BH multi-echo gradient-echo 3D Cartesian MRI and prototype FB multi-echo gradient-echo 3D stack-of-stars MRI at 3 T (MAGNETOM Skyra or Prisma, Siemens Healthineers, Erlangen, Germany) for abdominal fat quantification.[15] The 3D acquisitions in this study were performed in the axial orientation and prescribed primarily to cover the liver and typically included the pancreas as well. Depending on the subjects' breath-holding capabilities, the number of slices was reduced for BH Cartesian MRI compared to FB stack-of-stars MRI. Whenever possible, both acquisition methods used consistent parameters (Table 1). No interpolation was performed along the slice direction (i.e., reconstructed slice thickness matched the acquired slice thickness). BH Cartesian MRI was acquired at end-expiration. FB stack-of-stars MRI was reconstructed using data throughout the entire scan, without performing binning into separate respiratory motion states. 3D PDFF maps were calculated on the scanner from the multi-echo Cartesian and stack-of-stars MRI data using the same algorithm and a multi-peak fat model with a single R_2*.[28]

Image Analysis and pPDFF Measurement

In all subjects, the pancreas was contoured by a pediatric radiologist (12 years of experience, S.G.) by using a free-hand ROI tool (Horos software version 3.3.6, horosproject.org) on abdominal PDFF maps from FB stack-of-stars MRI, while using the first echo time images as anatomical references. The radiologist performed full segmentation of the pancreas (FS contours), and also placed 1-cm^2 oval ROIs within the pancreatic head, body, and tail for a total of 3 ROIs per subject. In addition, regional segmentation was obtained by the radiologist contouring the pancreatic head, body, and tail separately in each subject (Figure 1). Anatomic regions were defined as follows: the head is pancreatic tissue to the right of the superior mesenteric vein, the body is the medial half of remaining tissue outside the head, and the tail is the lateral half of remaining tissue outside the head. Cases where any anatomic regions of the pancreas were entirely excluded from available axial slices, or if excessive artifacts were present, were determined by the radiologist to be inadequate for pancreatic fat quantification. The pPDFF was measured from the FS, 3-ROI, and regional segmentation contours. Pancreatic volume was calculated by compiling the volume of each voxel included within FS and regional contours.

Comparing Free-Breathing and Breath-Holding MRI for pPDFF Quantification

In addition to analyzing the FB-MRI data, the radiologist also completed a set of FS and 3-ROI pancreatic contours in the corresponding BH-MRI PDFF maps (Figure 2). The measurements on BH-MRI were blinded to FB-MRI data.

Assessing Intra-Reader and Inter-Reader Agreement for FS and 3-ROI Pancreatic PDFF Measurements

To assess reader agreement for measuring pPDFF, a researcher (1 year of experience, J.D.S.) was trained and verified by the radiologist to serve as a second reader. Free-breathing MR images and PDFF maps were presented in a randomized and blinded fashion to the radiologist and the trained researcher with a minimum of two weeks between each session. Each reader measured FS and 3-ROI pPDFF independently. The measurement results were used to assess intra-reader agreement in FB-MRI pPDFF for each reader, as well as inter-reader agreement. pPDFF measured by the radiologist using the FS and 3-ROI methods were compared to determine differences between measurement methods.

Comparing Pancreatic PDFF Between Anatomic Regions

Pancreatic PDFF from regional segmentation on FB-MRI (Figure 1) was compared between each region (head, body, and tail) to determine if pPDFF differed between anatomic regions.

Relating Pancreatic PDFF to Clinical Markers of Metabolic Dysfunction

FB-MRI pPDFF data from the second set of the radiologist's FS and 3-ROI contours and from the only set of regional contours were used to assess relationships with anthropometric measurements and laboratory studies. Data from all subjects were used to relate FS, 3-ROI, and pancreatic head, body, and tail pPDFF with body composition (body mass index [BMI], BMI z-scores, and waist circumference) and liver PDFF, which was obtained through conventional BH-MRI to align with current clinical practice conventions. Because laboratory studies were not available for healthy subjects, pPDFF was correlated to serum liver function tests (aspartate aminotransferase [AST], alanine aminotransferase [ALT], alkaline phosphatase, and total bilirubin), hemoglobin A1c, and lipids (total cholesterol, low-density lipoprotein [LDL], high-density lipoprotein [HDL], triglycerides) in the overweight cohort only.

Statistical Analysis

Differences in continuous demographic, MRI, and clinical data were compared between the healthy and overweight cohorts using independent samples *t*-tests or Mann-Whitney U tests based on normality, as determined by the Shapiro-Wilk test. Differences in dichotomous demographic and clinical data were compared between cohorts using chi-squared tests.

Differences in pPDFF between FS and 3-ROI FB-MRI and BH-MRI measurements were assessed using the paired *t*-test or Wilcoxon signed-rank test depending on normality. Agreement in FS and 3-ROI pPDFF from FB-MRI and BH-MRI was assessed using Bland-Altman analysis to calculate the mean difference and 95% limits of agreement. In addition, the degree of agreement between FB-MRI and BH-MRI pPDFF was characterized using Lin's concordance correlation coefficient (CCC).[29]

Difference between FS and 3-ROI pPDFF was calculated using paired-samples *t*-test after confirming normality. Intra-reader agreement for FS and 3-ROI pPDFF measurements was determined using the intraclass correlation coefficient (ICC) with a two-way mixed effects model with single measurements to assess absolute agreement.[30] Inter-reader agreement

between measurements from the radiologist and the researcher was determined using the average pPDFF from two sets of tracings for each method, and calculated using ICC with a two-way random-effects model with multiple raters to assess absolute agreement.[30] Interpretation of ICC values was performed according to guidelines from prior literature (ICC < 0.5 reflects poor reliability, ICC between 0.5 – 0.75 reflects moderate reliability, ICC between 0.75 – 0.9 reflects good reliability, and ICC > 0.9 reflects excellent reliability).[30]

Differences of means between pPDFF and volume of different regions were calculated using one-way repeated measures analysis of variance with post hoc analysis. Spearman's rank correlation coefficients were used to assess the association between pPDFF and clinical markers. $P < 0.05$ was considered significant.

RESULTS

Participant Characteristics

This study enrolled 16 healthy children and 18 overweight children. Demographic information is summarized in Table 2. Healthy children (12.9 ± 2.8 years) were significantly younger than the overweight children (14.9 ± 2.4 years) and were less likely to be white (44% vs 89%) or Hispanic/Latino (19% vs 72%). Fifty percent of the overweight cohort had a previous diagnosis of prediabetes, and one subject had DM2. Compared to the healthy cohort, FS pPDFF in overweight children was significantly higher (15.1 ± 5.3% vs. 5.1 ± 1.7%). MRI data are summarized in Table 3.

Comparing Free-Breathing and Breath-Holding MRI for pPDFF Quantification

Image analysis was completed for all FB-MRI scans. Five BH-MRI scans did not include the pancreatic head, preventing both FS and 3-ROI contours from being placed. The BH-MRI scan for a single subject had excessive artifacts that prevented FS, but had sufficient coverage with no significant artifacts, which allowed for 3 ROIs to be placed. Therefore, FS tracings of the pancreas on BH-MRI were completed in 28 subjects and 3-ROI contours were completed on BH-MRI in 29 subjects. Among subjects with both FB-MRI and BH-MRI FS pPDFF measurements, pPDFF was comparable (BH: 9.3 ± 6.0% vs FB: 9.7 ± 6.1%, $p = 0.261$) with a mean difference of 0.41% with 95% limits of agreement of [−3.3%, 4.1%]; Lin's CCC was 0.95 [0.89 – 0.98]. Among subjects with both FB-MRI and BH-MRI 3-ROI pPDFF, results were also comparable (BH 3.7 ± 2.2% vs. FB 4.1 ± 2.8%, $p = 0.552$) with a mean difference of 0.40% with 95% limits of agreement of [−3.9%, 4.7%]; Lin's CCC was 0.62 [0.35 – 0.79]. The Bland-Altman plots are shown in Figure 3.

Assessing Reader Agreement for FS and 3-ROI Pancreatic PDFF Measurements

Radiologist measurements showed that pPDFF from the FS method was significantly higher than pPDFF from the 3-ROI method (data from second set of contours: FS pPDFF = 10.4 ± 6.4%, 3-ROI pPDFF = 4.2 ± 2.8%). For FS pPDFF, intra-reader agreement was excellent (ICC = 0.94 [0.88 – 0.97]). When using the 3-ROI method to measure pPDFF, intra-reader agreement was good (ICC = 0.82 [0.62 – 0.92]). Intra-reader agreement using data from the researcher and inter-reader agreement between the two readers are reported in Table S1

in Supplementary Information. Inter-reader agreement was good to excellent, though it was higher for 3-ROI pPDFF than FS pPDFF.

Comparing Pancreatic PDFF Between Anatomic Regions

Segmentation of each region of the pancreas showed that the volume of the pancreatic head (4.4 ± 0.7 cm^3) was significantly smaller than that of the body (15.9 ± 1.7 cm^3) and the tail (12.9 ± 1.3 cm^3), and the tail was significantly smaller than the body. The tail pPDFF (11.6 ± 8.1%) was significantly higher than that of the body (8.9 ± 6.3%) and head (8.7 ± 5.8%), but pPDFF of the body and head did not differ ($p > 0.999$) (Figure 4).

Relating Pancreatic PDFF to Clinical Markers of Metabolic Dysfunction

FS pPDFF positively correlated with BMI ($r = 0.73$), BMI z-score ($r = 0.76$), waist circumference ($r = 0.69$), and liver PDFF ($r = 0.78$) (Figure 5). Similar relationships were seen between these variables and 3-ROI pPDFF and pPDFF from each pancreatic region (Table 4). The degree of correlation was notably higher when using pPDFF from FS or from segmentation of the head (BMI: $r = 0.75$, BMI z-score: $r = 0.73–3$, waist circumference: $r = 0.67$, liver PDFF: $r = 0.83$), body (BMI: $r = 0.74$, BMI z-score: $r = 0.76$, waist circumference: $r = 0.71$, liver PDFF: $r = 0.79$), or tail (BMI: $r = 0.75$, BMI z-score: $r = 0.75$, waist circumference: $r = 0.72$, liver PDFF: $r = 0.78$) compared to pPDFF from the 3-ROI method (BMI: $r = 0.42$, BMI z-score: $r = 0.44$, waist circumference: $r = 0.38$, liver PDFF: $r = 0.52$), though all correlations were significant.

Within the overweight cohort, FS and 3-ROI pPDFF generally did not have significant correlations with liver function tests, hemoglobin A1c, or lipid levels. 3-ROI pPDFF correlated with serum ALT (Table 5). Hemoglobin A1c positively correlated with pPDFF of the pancreatic head ($r = 0.58$) and body ($r = 0.69$).

DISCUSSION

Free-Breathing MRI Facilitates Pancreatic Fat Measurement in Children

In this study, FB-MRI was used to acquire abdominal PDFF maps for the measurement of pancreatic fat in children. In subjects with adequate BH-MRI, FS pPDFF from FB-MRI and BH-MRI were in close agreement. 3-ROI pPDFF from FB-MRI and BH-MRI had lower Lin's CCC than FS pPDFF, which is likely attributable to the lower consistency of ROI placement that is inherent to the 3-ROI method, as reported in prior literature.[10] Because the subjects in this study did not undergo pancreatic biopsies, the accuracy of pPDFF from BH-MRI and FB-MRI could not be validated. However, a prior investigation in adults showed that pPDFF from BH-MRI correlated with the fat content of healthy tissue from pancreatic biopsies ($r = 0.80$, $p < 0.01$).[31] Since FB-MRI is easier to obtain and more child-friendly than BH-MRI,[11, 12] we propose that it may be a more compelling method to acquire pPDFF measurements for research and clinical purposes in children with metabolic dysfunction or other pediatric diseases known to affect the pancreas, such as pancreatitis,[32] Schwachman-Diamond syndrome,[33] cystic fibrosis,34 transfusion-related pancreatic siderosis,[18] and pancreatic exocrine dysfunction.[22]

Heterogeneity of Pancreatic PDFF Across Anatomic Regions

The finding that the pancreatic tail has more fat than other regions might be related to the anatomical location of the pancreas in the abdomen. Histologically, pancreatic fat is predominantly characterized by adipocyte infiltration rather than ballooning of parenchymal cells, which is observed in hepatic steatosis.[35] Therefore, the presence of adipose tissue surrounding different regions of the pancreas may directly relate to the amount of fat within that region. The tail of the pancreas is unique among pancreatic regions because it is located in the intraperitoneal space while the other regions are retroperitoneal. Because the peritoneum typically has a larger amount of fat compared to the retroperitoneum,[36, 37] the pancreatic tail may be more susceptible to adipocyte infiltration. Alternatively, the high pPDFF in the tail may reflect difficulties in excluding extra-pancreatic adipose tissue while performing FS tracings in superior axial levels. The actual mechanism(s) for regional variations of pancreatic fat remains unclear. These directions should be the topic of future investigations.

Utility and Limitations of Full Segmentation and 3-ROI Analysis Methods

Image analysis methods that inadequately sample the pancreas may systematically underestimate fat content by neglecting areas of high fat content. Indeed, the present study shows that pPDFF from the 3-ROI method was significantly lower than that from FS. This may suggest that the FS method is more likely to include regions that have higher fat, either because higher fat regions are closer to the edge of the pancreas and therefore would not be included if small ROIs are preferentially placed in the middle of each region, or because the reader had an inherent preference for placing small ROIs in low-fat areas. Indeed, pancreatic PDFF measured by the FS method had higher intra-reader agreement compared to the 3-ROI method, which was expected based on the substantially increased spatial extent of the FS tracings. On the other hand, the FS method may fail to exclude visceral fat surrounding the pancreas, leading to an overestimation of fat content. Inter-reader agreement was lower for FS than 3-ROI pPDFF, suggesting that difficulties in delineating the borders of the pancreas on all slices and excluding visceral fat may have decreased consistency between readers.

Another notable distinction between these methods is that 3-ROI weighs each region equally while FS weighs each region by their relative volumes. Since the pancreatic head has a smaller volume than the body and tail, the high-fat, high-volume tail region has a greater influence on FS pPDFF than 3-ROI pPDFF, which may contribute to the lower pPDFF from 3-ROI measurements. However, this alone may not fully account for the difference because regional segmentation of the lower-fat regions (head and body) produced a higher pPDFF than the 3-ROI method.

Clinical Context of Pancreatic PDFF from FB-MRI and the Benefits of Regional Analysis

The relationship between pancreatic fat and overall adiposity has been previously described. Some studies have associated pancreatic steatosis with BMI and body weight.[3, 5–7] In our study, pPDFF was positively correlated with BMI, BMI z-score, and waist circumference. This suggests that ectopic fat is deposited in the pancreas as adiposity increases. Increased pPDFF, in turn, may increase the risk for future insulin resistance and non-alcoholic fatty liver disease (NAFLD).

The notable differences between the FS and 3-ROI methods may contribute to inconsistencies among previous studies. For example, an investigation among overweight and obese adolescents found that pancreatic steatosis is a predictor of prediabetes,[2] but similar studies failed to find a relationship between pancreatic steatosis and insulin resistance.[3, 7] Studies that compared pancreatic fat with insulin sensitivity were similarly contradictory. Pacifico *et. al*[4] found a positive relationship with fasting insulin and pPDFF while Lê *et. al*[5] found no correlation. Furthermore, studies have assessed beta cell function by measuring responses to glucose loads. One study found that pancreatic fat predicted beta cell dysfunction.[6]

Our study noted relationships between pPDFF and serum ALT and hemoglobin A1c. Specifically, we observed relatively strong correlations between liver PDFF and pPDFF from FS and each region of the pancreas. The lowest correlation was observed between pPDFF measured by 3-ROI and liver PDFF. Notably, all subjects included in the overweight cohort had suspected or confirmed NAFLD. In contrast, a similar study of obese children with suspected or confirmed NAFLD failed to relate pPDFF to liver PDFF.[7] In adults, pPDFF has been shown to increase with increased liver steatosis.[20] When the present study's data were analyzed using specific regions of the pancreas, a positive correlation was noted between the head and body pPDFF and hemoglobin A1c. NAFLD and DM2 commonly coexist, and patients with diabetes are more likely to progress to non-alcoholic steatohepatitis (NASH), a more advanced form of NAFLD that can lead to liver failure.[38] These findings suggest that insulin resistance may play a role in liver fibrosis. When quantifying pPDFF it may be important to account for liver disease severity and specific pancreatic regions.

Limitations

Image acquisition in this study was limited to a single site, two MRI scanners, a single field strength, and a single vendor. This study was also limited by demographic differences between the healthy and overweight groups. Specifically, the overweight cohort was older and more likely to be white and Hispanic/Latino compared to the healthy cohort. As a result, the overweight cohort may have progressed further through puberty and have a different hormonal milieu. However, while pancreatic fat increases with age during childhood, this increase is proportional to increases in pancreatic parenchymal growth. Therefore, the fat percentage does not typically change during this time.[39] Many of the comparisons in this study were performed separately in healthy and overweight subjects, and BMI was analyzed using both raw BMI values and z-scores, minimizing the impact of this age discrepancy.[40] Agreement of pPDFF measured using FS and 3-ROI methods were assessed using two sets of contours from one pediatric radiologist and one trained researcher. Incorporating additional readers could strengthen this analysis. Because pancreas biopsies are rare in children, we could not validate pPDFF with histology, the gold standard. Lastly, laboratory data was not available for the healthy cohort.

Conclusion

FB-MRI pPDFF was in agreement with BH-MRI in a cohort of children, and FB-MRI pPDFF had good to excellent intra- and inter-reader agreement. The pancreatic tail has a

higher fat content than the body and head, and associations with insulin sensitivity and liver function vary between pancreatic regions. Future investigations of pediatric pancreatic fat may benefit from a regional analysis of pPDFF using FB-MRI.

Supplementary Material

Refer to Web version on PubMed Central for supplementary material.

Acknowledgements:

The authors thank the clinicians, study coordinators, and MRI technologists at UCLA for supporting this study.

Grant Support:

Research reported in this publication was supported by an Exploratory Research Grant from the UCLA Department of Radiological Sciences, the National Institute of Diabetes and Digestive and Kidney Diseases under Award Number R01DK124417, and the National Center for Advancing Translational Sciences under Award Number UL1TR001881. The content is solely the responsibility of the authors and does not necessarily represent the official views of the National Institutes of Health.

REFERENCES

1. Kumar S, Kelly AS. Review of childhood obesity: From epidemiology, etiology, and comorbidities to clinical assessment and treatment. Mayo Clinic Proceedings 2017;92:251–265. [PubMed: 28065514]
2. Toledo-Corral CM, Alderete TL, Hu HH, et al. Ectopic fat deposition in prediabetic overweight and obese minority adolescents. J Clin Endocrinol Metab 2013;98:1115–1121. [PubMed: 23386647]
3. Trout AT, Hunte DE, Mouzaki M, et al. Relationship between abdominal fat stores and liver fat, pancreatic fat, and metabolic comorbidities in a pediatric population with non-alcoholic fatty liver disease. Abdom Radiol 2019;44:3107–3114.
4. Pacifico L, Martino MD, Anania C, et al. Pancreatic fat and beta-cell function in overweight/obese children with nonalcoholic fatty liver disease. World J Gastroenterol 2015;21:4688–4695. [PubMed: 25914480]
5. Lê K-A, Ventura EE, Fisher JQ, et al. Ethnic differences in pancreatic fat accumulation and its relationship with other fat depots and inflammatory markers. Diabetes Care 2011;34:485–490. [PubMed: 21270204]
6. Maggio ABR, Mueller P, Wacker J, et al. Increased pancreatic fat fraction is present in obese adolescents with metabolic syndrome. J Pediatr Gastroenterol Nutr 2012;54:720–726. [PubMed: 22157928]
7. Kim J, Albakheet SS, Han K, et al. Quantitative MRI Assessment of Pancreatic Steatosis Using Proton Density Fat Fraction in Pediatric Obesity. Korean J Radiol 2021; 22:1886–1893. [PubMed: 34269534]
8. Sakai NS, Taylor SA, Chouhan MD. Obesity, metabolic disease and the pancreas—Quantitative imaging of pancreatic fat. Br J Radiol 2018;91:20180267. [PubMed: 29869917]
9. Yokoo T, Serai SD, Pirasteh A, et al. Linearity, Bias, and Precision of Hepatic Proton Density Fat Fraction Measurements by Using MR Imaging: A Meta-Analysis. Radiology 2018; 286:486–498. [PubMed: 28892458]
10. Kato S, Iwasaki A, Kurita Y, et al. Three-dimensional analysis of pancreatic fat by fat-water magnetic resonance imaging provides detailed characterization of pancreatic steatosis with improved reproducibility. PLoS One 2019;14:e0224921. [PubMed: 31790429]
11. Chavhan GB, Babyn PS, Vasanawala SS. Abdominal MR imaging in children: Motion compensation, sequence optimization, and protocol organization. Radiographics 2013;33:703–719. [PubMed: 23674770]

12. Courtier J, Rao AG, Anupindi SA. Advanced imaging techniques in pediatric body MRI. Pediatr Radiol 2017;47:522–533. [PubMed: 28409251]
13. Benkert T, Feng L, Sodickson DK, Chandarana H, Block KT. Free-breathing volumetric fat/water separation by combining radial sampling, compressed sensing, and parallel imaging. Magn Reson Med 2017;78:565–576. [PubMed: 27612300]
14. Armstrong T, Dregely I, Stemmer A, et al. Free-breathing liver fat quantification using a multiecho 3D stack-of-radial technique. Magn Reson Med 2018;79:370–382. [PubMed: 28419582]
15. Armstrong T, Ly KV, Murthy S, et al. Free-breathing quantification of hepatic fat in healthy children and children with nonalcoholic fatty liver disease using a multi-echo 3-D stack-of-radial MRI technique. Pediatr Radiol 2018;48:941–953. [PubMed: 29728744]
16. Ly KV, Armstrong T, Yeh J, et al. Free-breathing Magnetic Resonance Imaging Assessment of Body Composition in Healthy and Overweight Children: An Observational Study. J Pediatr Gastroenterol Nutr 2019;68:782–787. [PubMed: 30789865]
17. Chitiboi T, Muckley M, Dane B, Huang C, Feng L, Chandarana H. Pancreas deformation in the presence of tumors using feature tracking from free-breathing XD-GRASP MRI. J Magn Reson Imaging 2019;50:1633–1640. [PubMed: 30854767]
18. İdilman İS, Gümrük F, Haliloğlu M, Karçaaltıncaba M. The feasibility of magnetic resonance imaging for quantification of liver, pancreas, spleen, vertebral bone marrow, and renal cortex r2* and proton density fat fraction in transfusion-related iron overload. Turk J Haematol 2016;33:21–27. [PubMed: 26376710]
19. Yao WJ, Guo Z, Wang L, et al. Pancreas fat quantification with quantitative CT: an MRI correlation analysis. Clin Radiol 2020;75:397.e1–397.e6.
20. Patel NS, Peterson MR, Brenner DA, Heba E, Sirlin C, Loomba R. Association between novel MRI-estimated pancreatic fat and liver histology-determined steatosis and fibrosis in non-alcoholic fatty liver disease. Aliment Pharmacol Ther 2013;37:630–639. [PubMed: 23383649]
21. Beller E, Lorbeer R, Keeser D, et al. Hepatic fat is superior to BMI, visceral and pancreatic fat as a potential risk biomarker for neurodegenerative disease. Eur Radiol 2019;29:6662–6670. [PubMed: 31187217]
22. Kromrey M-L, Friedrich N, Hoffmann R-T, et al. Pancreatic steatosis is associated with impaired exocrine pancreatic function. Invest Radiol 2019;54:403–408. [PubMed: 30817380]
23. Hu HH, Kim H-W, Nayak KS, Goran MI. Comparison of fat-water MRI and single-voxel MRS in the assessment of hepatic and pancreatic fat fractions in humans. Obesity (Silver Spring) 2010;18:841–847. [PubMed: 19834463]
24. Staaf J, Labmayr V, Paulmichl K, et al. Pancreatic fat is associated with metabolic syndrome and visceral fat but not beta-cell function or body mass index in pediatric obesity. Pancreas 2017;46:358–365. [PubMed: 27941426]
25. Ogden CL, Carroll MD, Kit BK, Flegal KM. Prevalence of Childhood and Adult Obesity in the United States, 2011–2012. JAMA 2014; 311:806–814. [PubMed: 24570244]
26. American Diabetes Association: 2. Classification and Diagnosis of Diabetes: Standards of Medical Care in Diabetes—2019. Diabetes Care 2018; 42(Supplement_1):S13–S28.
27. Harris PA, Taylor R, Thielke R et al. Research electronic data capture (REDCap)—a metadata-driven methodology and workflow process for providing translational research informatics support. J Biomed Inform 2009;42:377–381. [PubMed: 18929686]
28. Zhong X, Nickel MD, Kannengiesser SAR, Dale BM, Kiefer B, Bashir MR. Liver fat quantification using a multi-step adaptive fitting approach with multi-echo GRE imaging. Magn Reson Med 2014;72:1353–1365. [PubMed: 24323332]
29. Lin LI-K. A Concordance Correlation Coefficient to Evaluate Reproducibility. Biometrics 1989;45:255–268. [PubMed: 2720055]
30. Koo TK, Li MY. A guideline of selecting and reporting intraclass correlation coefficients for reliability research. J Chiropr Med 2016;15:155–163. [PubMed: 27330520]
31. Fukui H, Hori M, Fukuda Y, et al. Evaluation of fatty pancreas by proton density fat fraction using 3-T magnetic resonance imaging and its association with pancreatic cancer. Eur J Radiol 2019;118:25–31. [PubMed: 31439250]

32. Acharya C, Navina S, Singh VP. Role of pancreatic fat in the outcomes of pancreatitis. Pancreatology 2014;14:403–408. [PubMed: 25278311]

33. Toiviainen-Salo S, Raade M, Durie PR, et al. Magnetic Resonance Imaging Findings of the Pancreas in Patients with Shwachman-Diamond Syndrome and Mutations in the SBDS Gene. J Pediatr 2008; 152:434–436.e2. [PubMed: 18280855]

34. Sequeiros IM, Hester K, Callaway M, et al. MRI appearance of the pancreas in patients with cystic fibrosis: a comparison of pancreas volume in diabetic and non-diabetic patients. Br J Radiol 2010; 83:921–926. [PubMed: 20965902]

35. Takahashi M, Hori M, Ishigamori R, Mutoh M, Imai T, Nakagama H. Fatty pancreas: A possible risk factor for pancreatic cancer in animals and humans. Cancer Sci 2018;109:3013–3023. [PubMed: 30099827]

36. Hung C-S, Lee J-K, Yang C-Y, et al. Measurement of visceral fat: should we include retroperitoneal fat? PLoS One 2014;9:e112355. [PubMed: 25401949]

37. Tanaka M, Okada H, Hashimoto Y, Kumagai M, Nishimura H, Fukui M. Intraperitoneal, but not retroperitoneal, visceral adipose tissue is associated with diabetes mellitus: a cross-sectional, retrospective pilot analysis. Diabetol Metab Syndr 2020;12:103. [PubMed: 33292449]

38. Anstee QM, McPherson S, Day CP. How big a problem is non-alcoholic fatty liver disease? BMJ 2011;343:d3897. [PubMed: 21768191]

39. Saisho Y, Butler A, Meier J, et al. Pancreas volumes in humans from birth to age one hundred taking into account sex, obesity, and presence of type-2 diabetes. Clin Anat 2007;20:933–942. [PubMed: 17879305]

40. Bell LM, Byrne S, Thompson A, et al. Increasing body mass index z-score is continuously associated with complications of overweight in children, even in the healthy weight range. J Clin Endocrinol Metab 2007; 92:517–522. [PubMed: 17105842]

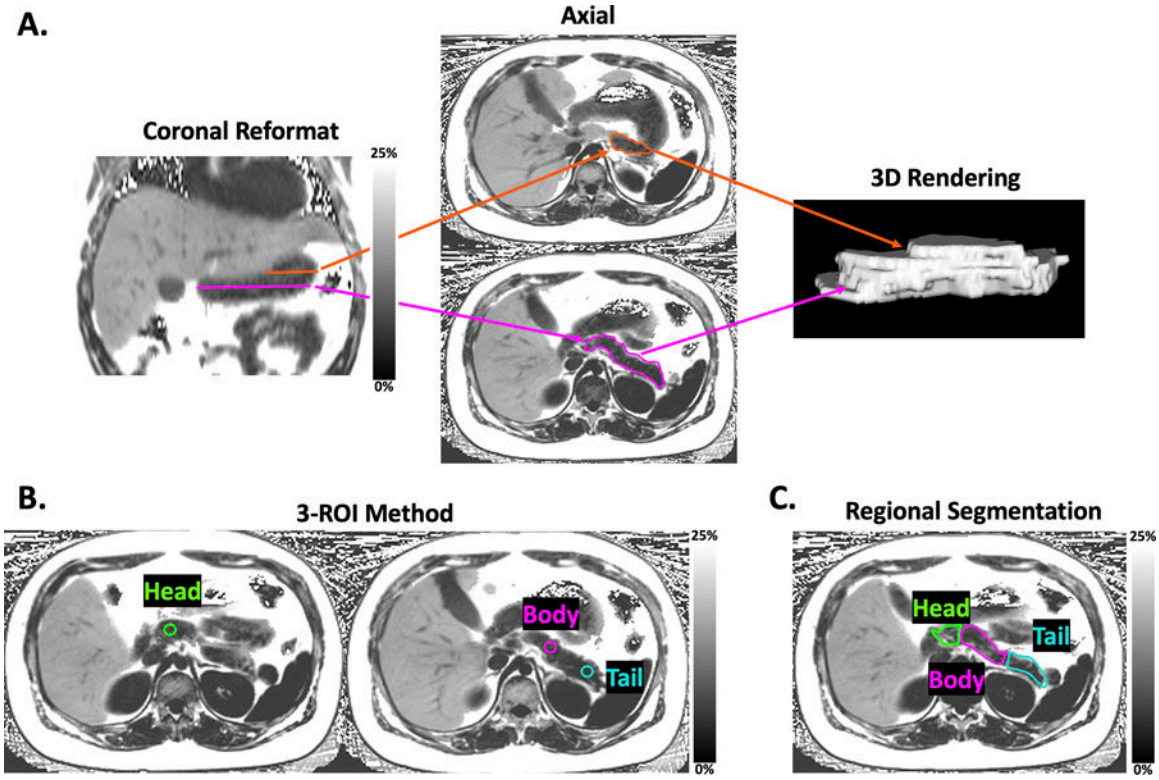

Figure 1. Image Analysis Methods to Measure Pancreatic Fat on MRI.

Representative examples of pancreatic segmentation in free-breathing MR images from an overweight subject (12 years old, male, BMI = 29.0 kg/m^2). **A:** Left: Coronal proton-density fat fraction (PDFF) map. Middle: Axial slices with full segmentation (FS) contours on PDFF maps. Right: 3D rendering of FS contours. **B**. 3-ROI method with 1-cm^2 ROIs placed in the head, body, and tail of the pancreas. **C.** Example of segmentation contours of each anatomic region (head, body, and tail) within the pancreas on an axial slice. Contours of each region were obtained at all axial levels of the pancreas, producing volumetric segmentation of each region.

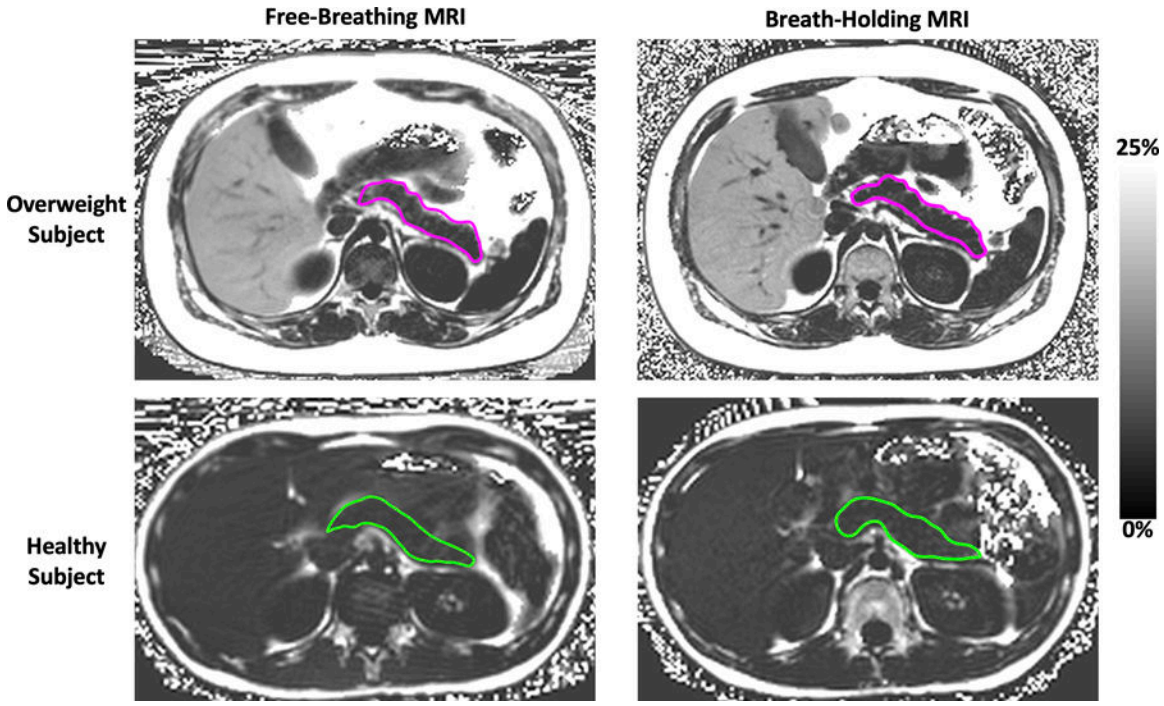

Figure 2. Free-Breathing vs. Breath-Holding MRI PDFF Maps With Pancreatic Contours.
Top row shows FB- and BH-MRI PDFF maps from a single overweight subject (12 years old, male, BMI = 29.0 kg/m^2). Bottom row shows FB- and BH-MRI PDFF maps from a single healthy subject (14 years old, male, BMI = 18.4 kg/m^2).

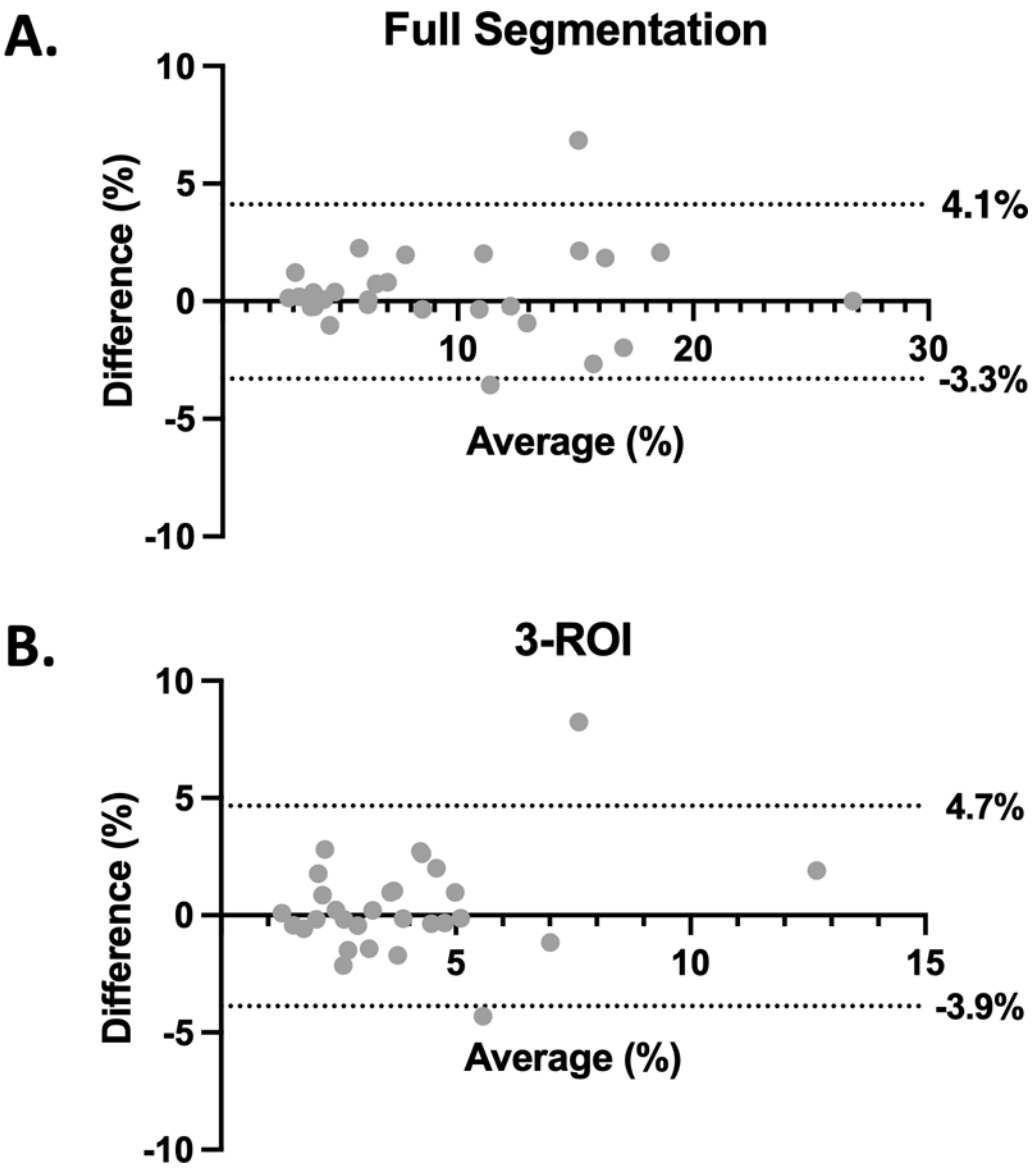

Figure 3. Bland-Altman Plots Comparing Pancreatic PDFF from Breath-Holding and Free-Breathing MRI.

A. Full segmentation was completed in FB- and BH-MRI for 28 subjects, and the mean difference was 0.41% with 95% limits of agreement of [−3.3%, 4.1%]. **B.** The 3-ROI method was completed in FB- and BH-MRI for 29 subjects, and the mean difference was 0.40% with 95% limits of agreement of [−3.9%, 4.7%].

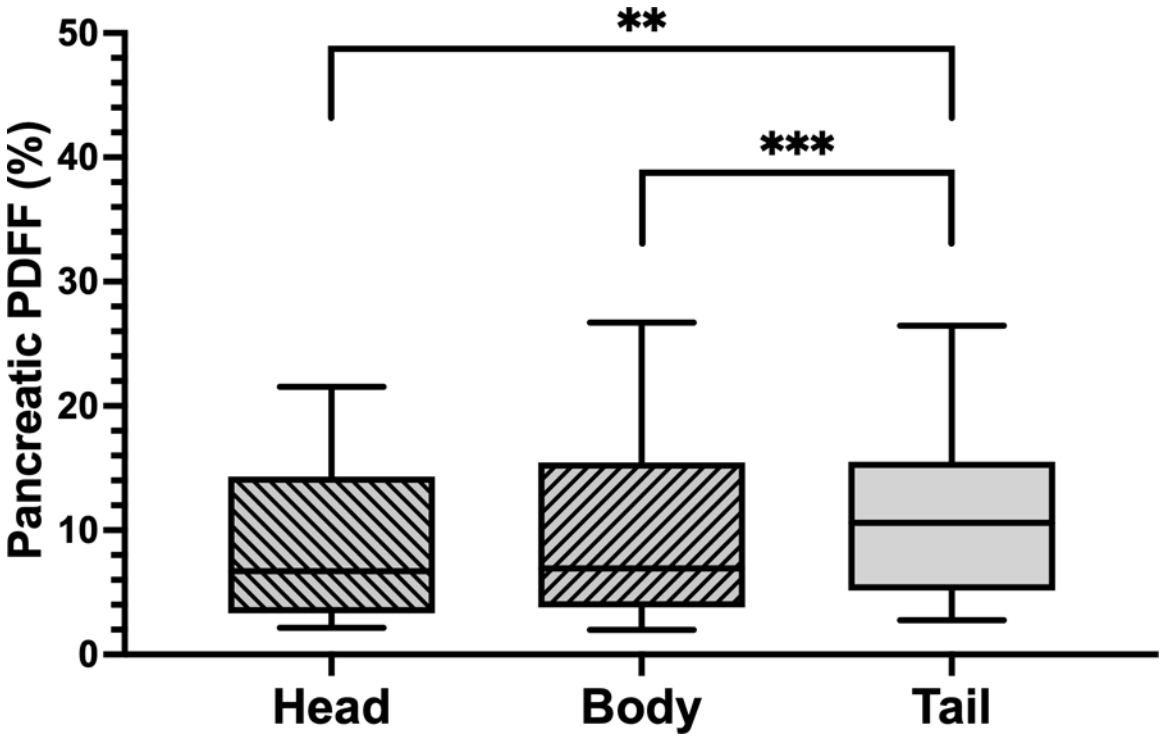

Figure 4. Pancreatic PDFF in Each Anatomic Region.

The tail region has significantly higher fat than the body or head. ** indicates $p < 0.01$ and *** indicates $p < 0.001$.

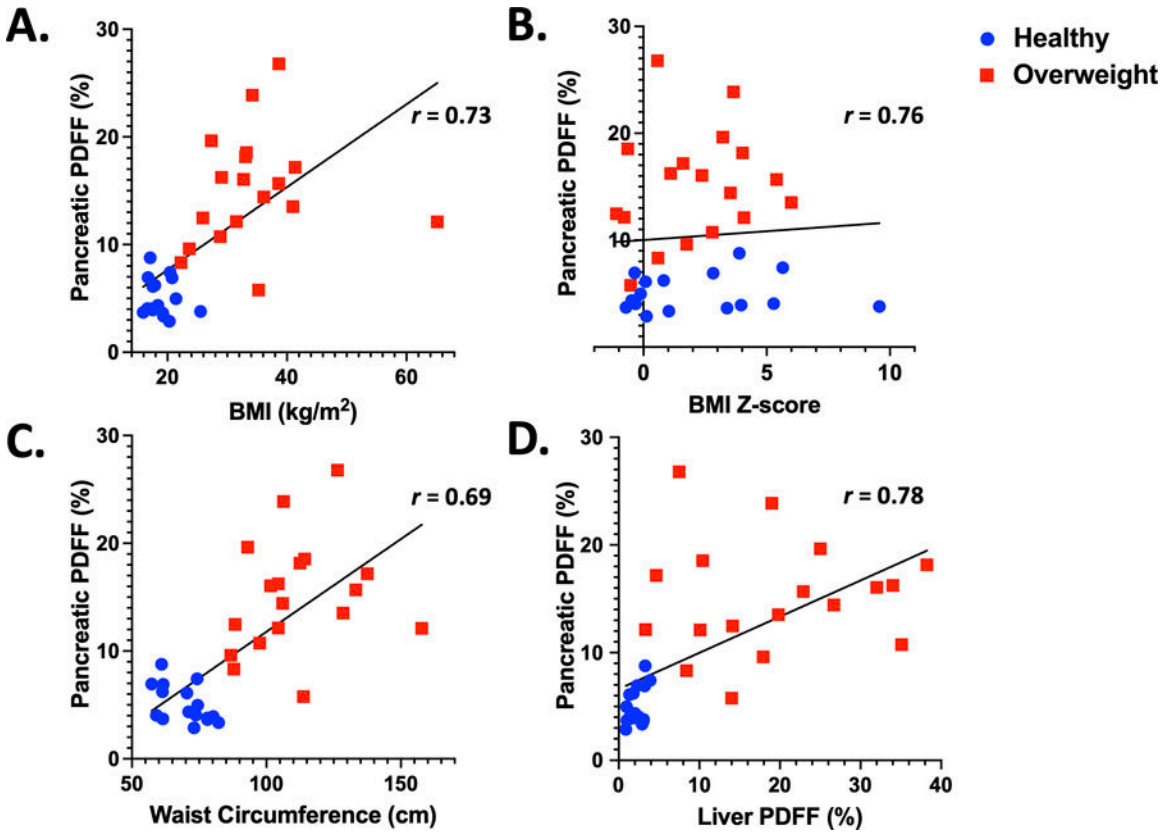

Figure 5. FS Pancreatic PDFF from FB-MRI Compared to Other Measures of Adiposity.

All correlations were performed with Spearman's rank correlation coefficient. **A.** FS pPDFF correlated with BMI. **B.** FS pPDFF correlated with BMI z-score. **C.** FS pPDFF correlated with waist circumference. **D.** FS pPDFF correlated with liver PDFF. All correlations were significant with $p < 0.001$.

Table 1.
Parameters for Breath-Held and Free-Breathing MRI at 3T.

Scans were acquired in the axial orientation.

	Breath-Held 3D Cartesian MRI	Free-Breathing 3D Stack-of-Stars MRI
Echo time (TE) (ms)	1.23, 2.46, 3.69, 4.92, 6.15, 7.38	1.23, 2.46, 3.69, 4.92, 6.15, 7.38
Repetition time (TR) (ms)	8.85	8.85
Matrix size [N_x, N_y]	160–288, 160–288	160–288, 160–288
Field-of-View [mm_x, mm_y]	280–500, 280–500	280–500, 280–500
Resolution [mm_x, mm_y]	1.67–1.94, 1.67–1.94	1.67–1.94, 1.67–1.94
Slice thickness (mm)	5	5
Bandwidth (Hz/pixel)	1080–1160	1080–1160
Number of slices	20–40	36–52
Radial spokes	N/A	252–453
Parallel imaging factor	4	N/A
Scan Time [min:sec]	0:16–0:25	2:09–4:43

Table 2.

Demographics.

All values reported as mean ± standard deviation where applicable. BMI: Body Mass Index. DM2: Type 2 Diabetes Mellitus.

	Healthy (N = 16)	Overweight (N = 18)	P Value
Age (years)	12.9 ± 2.8	14.9 ± 2.4	0.027
Male	8 (50%)	13 (72%)	0.291
White	7 (44%)	16 (89%)	0.009
Hispanic/Latino	3 (19%)	13 (72%)	0.003
BMI (kg/m^2)	18.9 ± 2.4	34.3 ± 9.5	<0.001
Waist Circumference (cm)	69.9 ± 8.3	111.1 ± 19.3	<0.001
Prediabetes Diagnosis	N/A	9 (50.0%)	
DM2 Diagnosis	N/A	1 (5.6%)	

Table 3.

MRI PDFF and Volume Data.

All values reported are from the radiologist measurements and are formatted as mean ± standard deviation where applicable. PDFF: proton-density fat fraction. pPDFF: pancreatic PDFF. BH: breath-holding. FB: free-breathing. FS: full segmentation method. 3-ROI: 3 regions of interest method.

	Healthy (N = 16)	Overweight (N = 18)	P Value
BH Liver PDFF (%)	2.2 ± 1.0	19.1 ± 10.9	<0.001
BH pPDFF, FS (%)	4.7 ± 1.4	14.6 ± 4.7	<0.001
FB pPDFF, FS (%)	5.1 ± 1.7	15.1 ± 5.3	<0.001
BH pPDFF, 3-ROI (%)	2.7 ± 1.0	5.0 ± 2.7	0.001
FB pPDFF, 3-ROI (%)	3.0 ± 1.6	5.3 ± 3.2	0.079
FB pPDFF, Head (%)	3.9 ± 1.7	13.0 ± 4.7	<0.001
FB pPDFF, Body (%)	4.1 ± 1.6	13.1 ± 5.9	<0.001
FB pPDFF, Tail (%)	5.5 ± 2.5	16.9 ± 7.5	0.042
FB Pancreas Volume, FS (cm^3)	28.3 ± 8.0	48.5 ± 24.6	0.001
FB Pancreas Head Volume (cm^3)	2.9 ± 2.1	5.8 ± 4.6	0.007
FB Pancreas Body Volume (cm^3)	11.2 ± 3.6	20.1 ± 11.6	0.042
FB Pancreas Tail Volume (cm^3)	9.2 ± 2.6	16.2 ± 8.9	0.005

Table 4.
Correlation Between PDFF of Each Pancreatic Region and Measures of Adiposity.

Spearman's rank correlation coefficients between pPDFF of each region of the pancreas and measures of adiposity. FS: full segmentation. 3-ROI: 3 regions of interest. BMI: body mass index. PDFF: proton-density fat fraction.

	Pancreatic Region				
	FS	**3-ROI**	**Head**	**Body**	**Tail**
BMI	0.73***	0.42*	0.75***	0.74***	0.75***
BMI z-score	0.76***	0.44**	0.73***	0.76***	0.75***
Waist Circumference	0.69***	0.38*	0.67***	0.71***	0.72***
Liver PDFF	0.78***	0.52**	0.83***	0.79***	0.78***

* indicates $p < 0.05$

** indicates $p < 0.01$

*** indicates $p < 0.001$

Table 5.

Pancreatic PDFF and Clinical Markers of Metabolic Dysfunction in Overweight Children.

r: Spearman's rank correlation coefficient. FS: full segmentation. Head: head region of the pancreas. Body: body region of the pancreas. Tail: tail region of the pancreas. AST: aspartate aminotransferase. ALT: alanine aminotransferase. LDL: low-density lipoprotein. HDL: high-density lipoprotein.

	Sample Size	FS pPDFF (r)	3-ROI pPDFF (r)	Head pPDFF (r)	Body pPDFF (r)	Tail pPDFF (r)
AST (U/L)	18	0.09	0.46	0.13	0.12	0.07
ALT (U/L)	18	0.18	**0.50** *	0.17	0.23	0.14
Alkaline Phosphatase (U/L)	17	−0.12	0.02	−0.05	−0.28	−0.19
Total Bilirubin (mg/dL)	17	0.24	0.48	−0.20	0.16	0.19
Hemoglobin A1c (%)	16	0.48	0.34	**0.58** *	**0.69** **	0.37
Total Cholesterol (mg/dL)	16	−0.11	0.27	−0.09	−0.24	0.20
LDL (mg/dL)	16	−0.06	0.25	−0.15	−0.20	0.22
HDL (mg/dL)	16	−0.22	−0.04	−0.35	−0.38	−0.13
Triglycerides (mg/dL)	15	0.19	0.50	0.44	0.31	0.46

* indicates $p < 0.05$

** indicates $p < 0.01$